

An Overview of Microrobotic Systems for Microforce Sensing

Georges Adam,¹ Mokrane Boudaoud,²
Valentin Reynaud,³ Joel Agnus,³
David J. Cappelleri,^{1,4} and Cédric Clévy³

¹School of Mechanical Engineering, Purdue University, West Lafayette, Indiana, USA;
email: dcappell@purdue.edu

²Institut des Systèmes Intelligents et de Robotique, UMR 7222, Sorbonne University,
Paris, France; email: mokrane.boudaoud@sorbonne-universite.fr

³FEMTO-ST Institute, University of Franche-Comté and École Nationale Supérieure de
Mécanique et des Microtechniques (SUPMICROTECH-ENSMM), CNRS UMR 6174,
Besançon, France; email: cedric.clevy@femto-st.fr

⁴Weldon School of Biomedical Engineering, Purdue University, West Lafayette, Indiana, USA

ANNUAL REVIEWS CONNECT

www.annualreviews.org

- Download figures
- Navigate cited references
- Keyword search
- Explore related articles
- Share via email or social media

Annu. Rev. Control Robot. Auton. Syst. 2024.
7:359–83

First published as a Review in Advance on
January 2, 2024

The *Annual Review of Control, Robotics, and Autonomous Systems* is online at
control.annualreviews.org
<https://doi.org/10.1146/annurev-control-090623-115925>

Copyright © 2024 by the author(s). This work is licensed under a Creative Commons Attribution 4.0 International License, which permits unrestricted use, distribution, and reproduction in any medium, provided the original author and source are credited. See credit lines of images or other third-party material in this article for license information.



Keywords

microforce sensing, microforce measurement, microrobotics, calibration, characterization, micromanipulation

Abstract

Considering microrobotics, microforce sensing, their working environment, and their control architecture together, microrobotic force-sensing systems provide the potential to outperform traditional stand-alone approaches. Microrobotics is a unique way for humans to control interactions between a robot and micrometer-size samples by enabling the control of speeds, dynamics, approach angles, and localization of the contact in a highly versatile manner. Many highly integrated microforce sensors attempt to measure forces occurring during these interactions, which are highly difficult to predict because the forces strongly depend on many environmental and system parameters. This article discusses state-of-the-art microrobotic systems for microforce sensing, considering all of these factors. It starts by presenting the basic principles of microrobotic microforce sensing, robotics, and control. It then discusses the importance of microforce sensor calibration and active microforce-sensing techniques. Finally, it provides an overview of microrobotic microforce-sensing systems and applications, including both tethered and untethered microrobotic approaches.

1. INTRODUCTION

Microscale applications:

applications involving objects or components at the micrometer scale

For 30 years, microrobotics has been considered a scientific field of its own, because it provides original tools and methods able to achieve tasks at the micrometer scale. This scale is characterized by objects of interest with at least one dimension of less than 1 mm (which not only limits manual intervention by a human operator but also comes with numerous application requirements), and microrobotics provides a unique and novel ability for humans to interact with such objects. These interactions appear to be highly useful for the purposes of characterization and control in manipulation and assembly tasks. Many robots have been developed and bring the ability to set several key parameters of this interaction (**Figure 1**). How to control the interaction between a robot and its environment (biological objects, synthetic components, tissues, etc., generally referred to as samples) remains at the same time an open question and central to the success of most tasks. In fact, the problem of controlling these interactions deals with several interrelated issues specific to the microscale, as shown in **Table 1**.

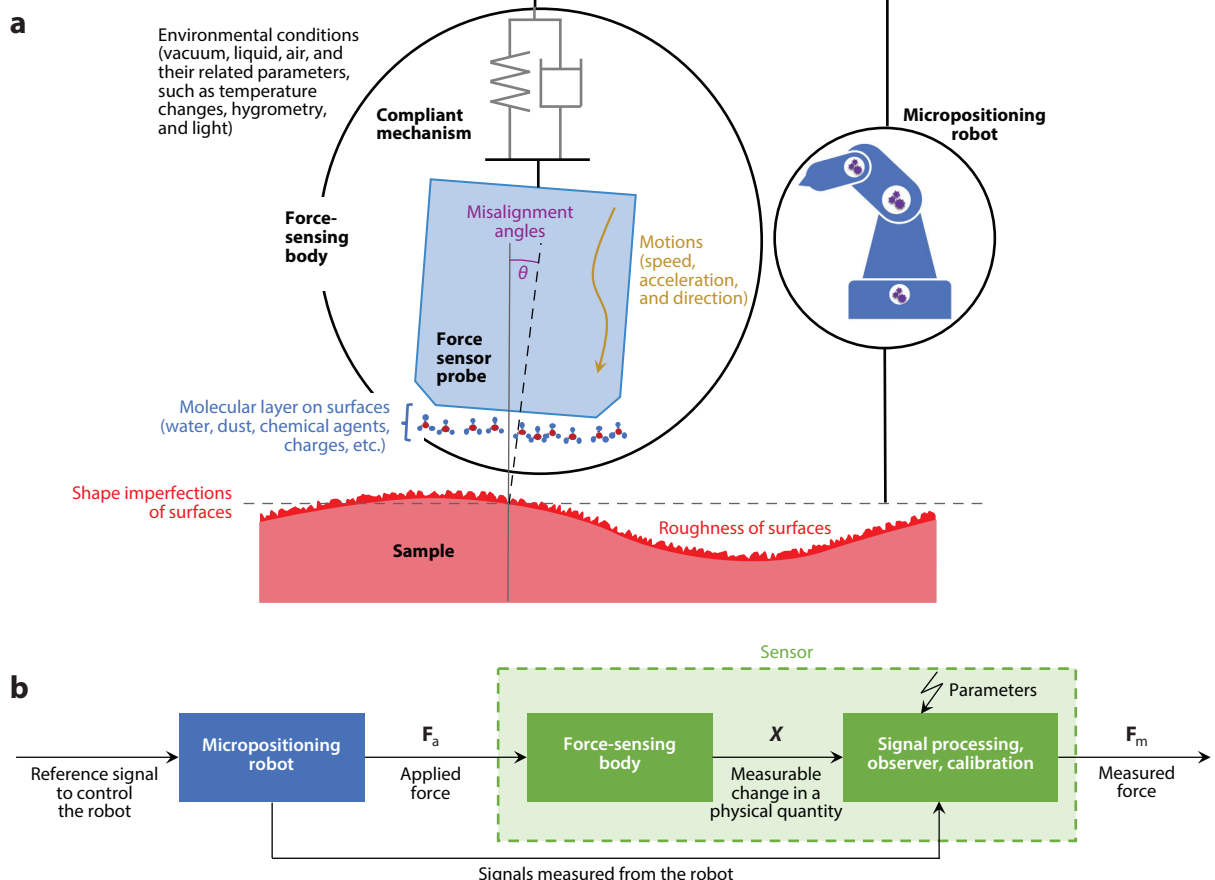


Figure 1

(a) Influential parameters for microforce sensing with robots. (b) Schematic showing the principles of microforce sensing with robots. A micropositioning robot generates a relative motion between the force sensor probe and a microscale sample that induces a force (F_a) to be measured (F_m).

Table 1 Main challenges of microforce measurement at the microscale

Microscale characteristics	Consequences for microforce sensing
Local physical effects (electrostatic, surface force predominance, etc.)	<ul style="list-style-type: none">■ Fast motion around the contact between the sample and force-sensing body (pull-in and/or pull-off effects)■ Unwanted relative motions between the sample and the force-sensing body
Environmental parameters (e.g., temperature and humidity)	<ul style="list-style-type: none">■ Drift of measurements■ Increase in standard deviation■ Loss of measurement traceability
Imperfect motions generated by the robot (nonlinear actuation, geometrical imperfections, backlash, and closed-loop induced delays)	<ul style="list-style-type: none">■ Introduction of additional influential parameters to measurements■ Increase in standard deviation■ More complex analysis of influential parameters
Compliance of the measuring instrument on the same order of the sample	<ul style="list-style-type: none">■ Difficulty in separating the properties of the sample from those of the instrument
High dynamics of objects	<ul style="list-style-type: none">■ Unwanted and/or uncontrolled vibrations■ Sensor noise■ High bandwidth in measurement and control

In this context, force sensing has emerged as a key technology to measure forces occurring between a robot and a sample. Although macroscale force sensing is a widely studied and developed field, its methods cannot be directly applied to microscale applications. Many of the constraints in microforce sensing stem from the reduced size scale and high-resolution requirements. Other important considerations, depending on the force-sensing method, may include possible microfabrication difficulties, sensor noise, or temperature and electrostatic effects. Some of the main challenges associated with microforce sensing are due to the small footprints required and difficult fabrication procedures. Additionally, the signal-to-noise ratio can be poor for some sensor types and is often highly dependent on environmental conditions. Despite these challenges, many microforce sensors have been designed by researchers, as demonstrated by several survey papers (1–5), and multiple companies have brought microforce sensors to the market—FemtoTools (Switzerland), TEI (France), THK Precision (Japan), Honeywell (USA), Kleindiek (Germany), Bruker (USA), and CLA (Switzerland).

However, the effective use of force sensors for microscale applications is not straightforward and presents several challenges. First, microforce sensing cannot be carried out directly and requires deforming a force-sensing body (**Figure 1a**). Micropositioning robots are generally used to control the position, speed, acceleration, and relative angles of the sensor body before and after the contact with the sample. The robot is thus a critical part of the measurement chain and greatly influences the efficiency of the force measurement. For instance, it can compensate for misalignment, drift, and other measurement system uncertainties. Hence, most of the time, microforce sensing cannot be done with the sensor alone; it also requires consideration of the micropositioning robot. Second, the force-sensing body, when being deformed by the robot, provides a measurable change in a physical quantity such as strain or displacement. This change is used to provide the measured force (F_m), which is an estimate of the force applied by the robot (F_a), as shown in **Figure 1b**. To obtain microforce sensing that matches application requirements, the range, resolution, bandwidth, and accuracy directly depend on the way this estimation is done. Dynamic modeling of the force-sensing body, automatic control methods, data processing, and sensor calibration must also be considered in the process of microforce sensing. With these aspects in mind, this article presents the state of the art in microforce sensing, where the microforce sensor, the microrobotic system, the control, and the signal processing are included in a complete measurement chain operating in a specific environment (**Figure 1**).

Microfabrication:
the set of manufacturing techniques used to produce devices with structures at the micrometer scale and below

Microforce sensors:
sensors able to measure forces acting at the micronewton scale

Micropositioning robots: robots with at least three degrees of freedom that are able to achieve positioning tasks at the micrometer scale

In this article, Section 2 presents some of the fundamentals of microforce sensors, including their performance and the physical principles on which they are based. Section 3 deals with an overall picture of robotic issues for force generation and sensing as well as the associated control strategies. Section 4 is dedicated to microforce sensor calibration issues. Section 5 introduces active sensing, which is a specific case where actuation and control play a fundamental role in force-sensing performance. Section 6 introduces state-of-the-art microrobotic systems used for micro-force sensing and the main applications. Finally, some conclusions are presented in the last section.

2. MICROFORCE SENSING: MAIN PRINCIPLES AND METHODS

Despite the challenges related to microforce sensing, multiple types of sensors have been used to achieve micronewton-level force measurement, each with its own advantages and disadvantages, as discussed in this section. They include vision-based, capacitive, piezoresistive, piezoelectric, optical, and field-based force-sensing techniques, among others. The goal of this section is to focus on the most popular methods employed for microforce sensing and possible integration with microrobots.

To compare different microforce-sensing methods, several key sensor properties—including resolution, range, and trueness, among others—must be properly defined. In this review, resolution is defined as the smallest change in measured force detected by the sensor in question, range is defined as the latitude of forces in which the sensor can reliably measure them, and trueness refers to how accurate the sensor is (i.e., how closely the measured value relates to the actual force). As discussed further in this section, there are many challenges in microforce sensing, and one of them is the lack of standardized definitions for these terms and a concrete way to compare different sensors. Using the definitions above, we contrast different types of microforce sensors, highlighting their specific advantages and disadvantages. Other considerations that must be taken into account when comparing different force-sensing methods include their sensitivity to environmental conditions (e.g., temperature and humidity), their measurement noise susceptibility, the frequency response of the measurement, and the complexity of the required experimental setup (circuitry, overall footprint, and necessary filters).

Figure 2 compares the methods in more detail, while **Figure 3** provides a range-to-resolution representation of available microforce sensors. The latter shows that commercial sensors are widely used for measurement ranges greater than 10 mN; between 100 μ N and 10 mN, numerous sensors have been proposed by researchers, with substantial challenges around the measurement range-to-resolution ratio as well as the number of measurement axes; and very few solutions allow measurement ranges below 100 μ N.

Capacitive force sensors work by measuring the change in capacitance in the device, which can be directly linked to an applied force. In the simplest capacitive sensors, a set of conductive parallel plates insulated from each other, usually with a dielectric material between them, is used as the main sensing body. Therefore, when a force is applied to the system, these parallel plates move relative to each other. This results in a change of mutual capacitance, which is measured, and the applied force is computed from it. This same effect is utilized in modern accelerometers, which use parallel plates attached to a proof mass system. This type of force sensor is extremely popular (9, 12, 41) since it can measure forces in a wide range, from the millinewton to the piconewton range. Additionally, it provides a good frequency response, is not very sensitive to environment changes (such as changes in temperature or humidity), and requires very low energy to operate. On the other hand, capacitive force sensors are highly susceptible to noise, often requiring complicated circuitry for normal operation and to filter out the noise. This can result in slightly larger footprints that can prove hard to integrate into other microsystems.

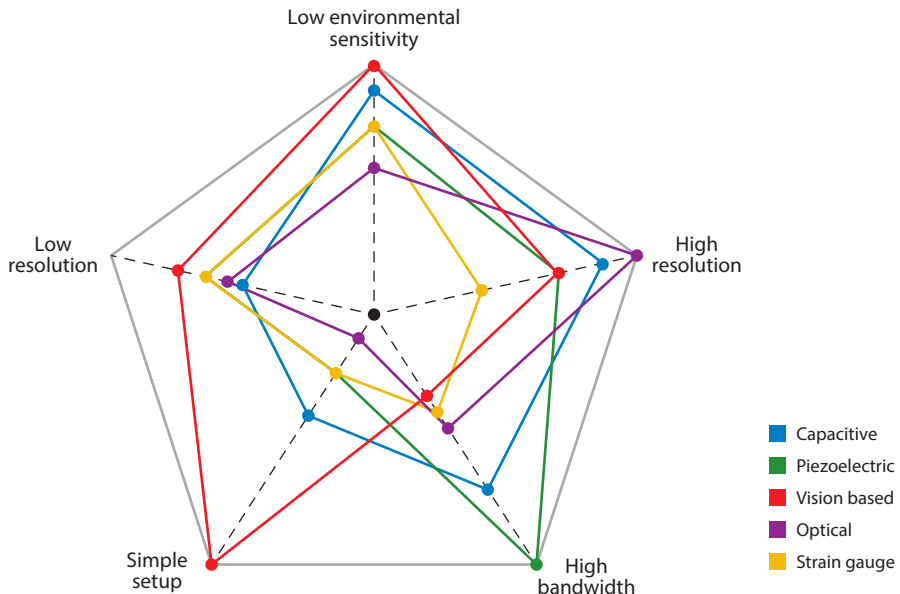


Figure 2

Schematic comparing different working mechanisms of commonly used force sensors for measurements at the microscale and below. Points farther away from the center denote better characteristics in that metric.

Strain gauge force sensors are another common approach for sensing. As force is applied to the sensor's structure, deformations occur according to Hooke's law, resulting in a change of resistance, which enables the applied force to be calculated. We can distinguish two subgroups: metallic and piezoresistive strain gauges. The metallic ones exhibit a change of resistance according to the strain mainly because of geometrical modification (elongation and contraction). On the other hand, piezoresistive sensors utilize a change of the resistivity of the material (piezoresistive effect) to compute forces. The gauge factor (G) is a metric that corresponds to the ability of the material to have a change in resistance (ΔR) based on its deformation (ε). This factor is defined as $G = \Delta R / (R \cdot \varepsilon)$. Metallic strain gauges allow a gauge factor from 2 up to ~ 5 for platinum. Piezoresistive strain gauges offer greater gauge factors, from approximately 20 for polysilicon up to 100–200 for silicon depending on the doping concentration and whether the material is P or N type.

Metallic strain gauge force sensors are popular due to their simplicity and low cost (42, 43). Additionally, they provide a sensing range around the millinewton level and have been deeply studied. These sensors can also be susceptible to environmental conditions (e.g., temperature and humidity), can present elevated noise levels, and need a Wheatstone bridge to amplify the quite small resistance changes and simultaneously amplify the noise. Piezoresistive strain gauge sensors (24, 44) are also widespread for force sensing, since they have a relatively simple working principle. However, they need specific clean room facilities for fabrication, making them more complex to fabricate and usually more expensive. Thanks to their larger gauge factor, piezoresistive strain gauges have a wider sensing range, usually around the millinewton to sub-millinewton level. Similarly to metallic sensors, piezoresistive gauges also typically require a Wheatstone bridge; however, a lower amplification gain is needed, resulting in a more favorable signal-to-noise ratio and expected stroke and resolution. As the piezoresistivity can be considered an instantaneous effect, the dynamic performance of such a sensor is directly linked to the dynamic capability of the compliant

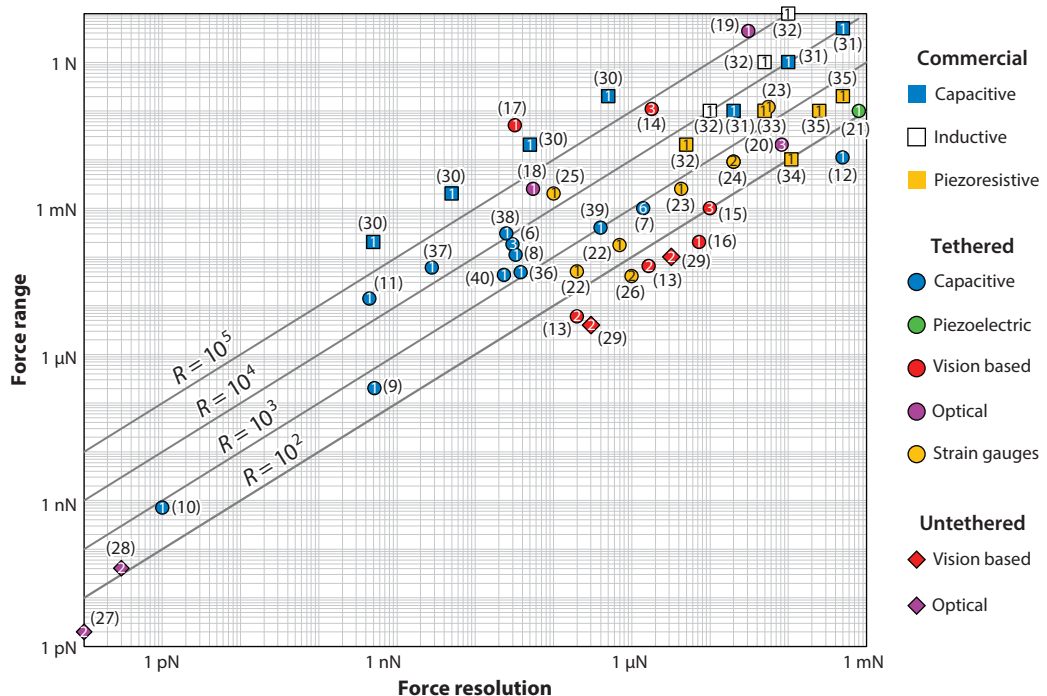


Figure 3

Microforce sensors available commercially or in the literature, showing a range-versus-resolution plot along with their working principle. The numbers inside the various shapes refer to the number of measurement axes, and R is the range-to-resolution ratio. For commercially available sensors, the performance evaluation usually considers the sensor and its signal conditioning unit as well as its signal processing unit; for sensors from the literature, the evaluation considers only the sensor and its signal conditioning unit.

mechanism (deformation body) of the sensor that integrates the gauges. Despite these benefits, this kind of sensor still faces some issues when it comes to miniaturization of its footprint and attachment to different test beds. Furthermore, some materials that present the piezoresistive effect, like silicon, can be extremely brittle, making some force measurements difficult.

Piezoelectric sensors are able to compute applied forces by measuring the changes in electrical charge that occur due to mechanical deformation, a property of the direct piezoelectric effect (21, 45). The most attractive feature of these sensors is their high frequency response, making them the optimal solution for measuring microdynamic systems. Furthermore, piezoelectric sensors are usually small, have high sensitivity, and have a relatively simple structure. However, these sensors are unable to measure static forces and cannot operate in high temperatures, and charge leakages can occur, resulting in some measurement drift over time and lower reliability.

Optical technology has been used in multiple ways to achieve microforce sensing (46–49), including in laser Raman spectroscopy techniques and a laser interferometer method, among others. One notable optical force-sensing technique is the use of optical tweezers for measurement. Here, a focused light beam creates an optical trap in which a force is always exerted on the trapped particle toward the center of the beam. When an external force is applied to the particle, its position deviates from the center of the optical trap, enabling the calculation of the exerted force based on this deviation. Utilizing this sensing method enables a wide sensing range at the piconewton level, but large costs are usually associated with it, and there are limitations regarding the types of particles that can be used for force sensing.

In contrast to optics-based microforce sensors, vision-based sensors utilize images taken at different times along with a computer vision algorithm of some sort to process them and compute forces (27, 29, 50). In most cases, the algorithm tracks the deflection of a structure of known stiffness, and Hooke's law is then applied to compute the force. Using this method enables sub-micronewton resolution while maintaining the high flexibility of the sensor, which is able to be incorporated into a wide range of test beds due to its simplicity. Furthermore, the fact that it does not require any onboard electronics or a large footprint enables its use for wireless microrobots and other small-scale systems. A few disadvantages of this sensor type include the trade-off between resolution and field of view (depending on the camera's zoom level) and the fact that if an object blocks the view of the camera, force sensing is no longer possible. With the development of higher-speed cameras and better discrete-event cameras, this method is gaining traction and has a promising future in microforce sensing for microrobotics.

3. ROBOTICS AND CONTROL TO MEASURE AND APPLY FORCES

Different solutions exist to create motions, deformations, or displacement. The main ones are tethered and untethered microrobotic systems (see Section 6.1). All of these technologies are of high interest for microforce sensing because they generate and control motions with enough degrees of freedom (DOFs), resolutions, and bandwidths to deal with the specificities of the small scales. They are also useful to set important parameters, such as the speed or acceleration of the motion, which is important to consider during a force measurement.

Several control schemes have demonstrated their abilities to control position, deformation, or forces either in open or closed loop (51). Downscaling leads to a reduction in the mass of objects and thus to an increase in their bandwidth. This raises several issues concerning the choice of hardware used for the control loop (real-time boards, field-programmable gate arrays, etc.) and for acquisition (the need for instruments with suitable bandwidth). The increase in bandwidth, coupled with the low orders of magnitude of the signals, implies a low signal-to-noise ratio. Manufacturing techniques lead to uncertainties in the dimensions of microrobotic systems, implying uncertainties in their models. Finally, the actuator nonlinearities most commonly encountered at small scales are hysteresis and creep, which are consequences of the widespread use of piezoelectric materials for actuation and measurement. For this reason, a branch of automation is focusing on the control of small-scale systems through the design of control laws robust to uncertainties, nonlinearities, and noise (52).

Particularly for force measurement, estimation, and control, one can rely on techniques and methods for observation, regulation and disturbance rejection. Observation aims to estimate a force that cannot be measured directly. It often relies on the system model (e.g., the robot or force sensor). The Luenberger state observer is one of the most widely used for linear time-invariant systems. Its inputs are the system input and output, and its output is the signal to be estimated (**Figure 4a**). When measurements are noisy in the bandwidth of interest, the Kalman filter is a well-suited approach. This filter has been used in several microrobotics applications when a force has to be measured despite vibration and noises (53, 54). The disturbance observer is another structure that allows the estimation of a disturbance that affects the system (55). Thanks to this estimation, the perturbation can be rejected with an appropriate controller. Regulation is needed when the force has to be controlled. This is mainly the case for gripping force, contact force, and breaking force. There are mainly two control strategies: feedback and feedforward (**Figure 4b,c**). The former is preferred because of its robustness, but it is not always applicable, especially when the force cannot be measured directly. In this case, the feedforward controller is useful, but it requires a well-modeled system (56).

Tethered microrobotic system:
a microrobotic system whose base and tip (end effector) are physically attached by a tether

Untethered microrobotic system:
a microrobotic system whose base and tip (end effector) are not physically attached; the end effector is moved using external fields that act at a distance, such as magnetic fields

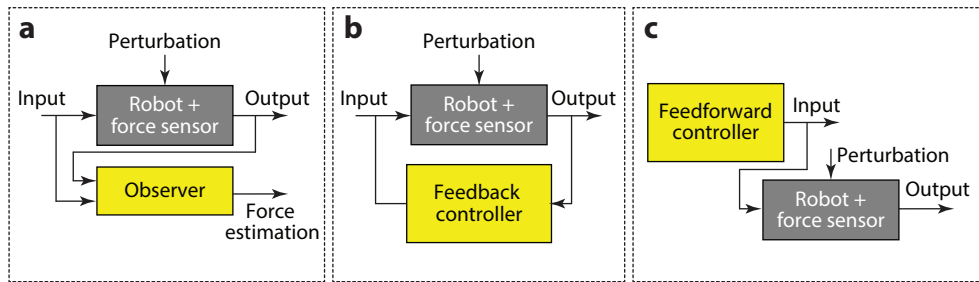


Figure 4

Schematic views of (a) force estimation with an observer, (b) force regulation with a feedback controller, and (c) force regulation with a feedforward controller.

An explicit force control scheme is especially well suited to dynamically controlling forces that change between the force-sensing body and the sample (i.e., where there is always a contact between them) (57). Nevertheless, for most applications, contacts between the force-sensing body and its environment are intermittent. In this case, free motion and constrained motions alternate, requiring a switch between position and force control (58). Control schemes enabling an efficient and smooth switch between them are available. During these alternating states, achieving force measurement at the microscale usually requires considering adhesion forces when contact occurs or when two surfaces come close together (i.e., typically within a few hundred nanometers). These forces induce nonlinear behaviors usually known as pull-in and pull-off effects, making control methods, such as impedance-based control that is able to dynamically control contacts, very important at the microscale (59–61). Robot control methods are also important to adapt to changes in environmental parameters such as temperature or humidity, which are always influential at the microscale even in well-controlled environments (62).

Robots also bring multi-DOF capabilities that allow for several key advantages. First, they enable the relative motion between a force-sensing body and the sample to be characterized. This is useful to accurately select the point or area where the force has to be measured. This multi-DOF capability also enables the control of several important parameters, such as the contact angles and relative orientations of motions or surfaces. Nevertheless, an increase in the number of DOFs is always accompanied by an increase in the effects from imperfections in the robotic structure (63). It is possible, for instance, to measure and compensate for imperfections such as perpendicularity errors between axes by using robot calibration (64). However, achieving force sensing by robots at the microscale requires considering many more imperfections. Indeed, robots used for microforce sensing are very large compared with the volume of interest even if their motions have very high resolutions (typically nanometer level). Their imperfections can be substantial, inducing poor repeatability and accuracy (65). For instance, robotic stages used to achieve translation do not really succeed in moving along a straight line due to yaw, pitch, and roll parasitic motions, which are themselves induced by the mechanical guidance of the stages. Additional imperfections are also introduced by actuators whose physical principles generate vibrations. Also, even if most of the stages embed their own sensors, enabling closed-loop control at the joint level, this control has limited interest when the sensor provides indirect measurement of the motion (66).

Many robots have come from the concatenation of several elementary translation and/or rotation stages, resulting in stacking and increases of these imperfections. Several studies have recently been done showing that robot calibration methods can significantly improve the positioning accuracy of such robots for microscale (67–70) and nanoscale (65, 71) purposes. These methods consider both intrinsic (building and configuration of the robot) and extrinsic (relative positions

of the robot, sensor, and environment frames) parameters that can be identified to compensate for the effects of these imperfections (72). The difficulty in achieving local and multiaxis measurement at the microscale makes this an active research topic despite the promising methods that have already been investigated.

4. MICROFORCE SENSOR CALIBRATION

The calibration process is a crucial step in the development of every transducer, where the correspondence between the force F_a applied by a reference and the measured force F_m (**Figure 1b**) is identified and experimentally validated with a specific calibration setup and procedure. To obtain an accurate calibrated sensor, a key element is the definition of the reference used. Three main principles are considered in the literature (73): calibrated cantilevers, other calibrated sensors, and microbalances.

A calibrated cantilever can be used as a force reference by measuring its bending and knowing its stiffness, as exemplified in **Figure 5a**. This technique is used when the deflection of the reference can be precisely determined during the force application. Frühauf et al. (76) considered this technique suitable for a force sensor with a precise external position measurement, as is the case for scanning probe microscopy instruments like atomic force microscopes (77). If 1% uncertainty can be reached, the trueness of the values will strongly depend on several parameters, such as the position of the contact point and the Young modulus, leading in reality to more than several percentage points of uncertainty (78).

The use of another microforce sensor, such as the one shown in **Figure 5b**, as a reference is quite widespread to calibrate a different microforce sensor (17, 79–81). Jang et al. (82) calibrated a set of biocompatible sensitive SU-8 cantilevers with piezoresistive glass-like carbon gauges using a commercially available and calibrated capacitive microforce sensor (the FemtoTools FT-S1000). The variation of the output signal from the gauge is compared with the value of the reference from 150 μN to 8 mN with 20- μN static steps, actuated by a precise positioner. This way, bending can be approximated and then stiffnesses computed, from 6.3 to 72 N/m. The same calibrated sensor was used by Tiwari et al. (24) to characterize a microgripper with mounted piezoresistive silicon gauges. Tests are done from 0 to 9 mN, resulting in a 9-mN range and a calibrated stiffness of 5,130 N/m.

These sensors have been calibrated using microbalances and measurement methods (**Figure 5c,d**) studied by national metrology institutes that, in particular, investigate the notion of metrological traceability, which is defined as the “property of a measurement result whereby the result can be related to a reference through a documented unbroken chain of calibrations, each contributing to the measurement uncertainty” (83, p. 29). Indeed, at the macroscale, standard processes exist to ensure the traceability of instruments, such as the ISO 376:2011 standard for axial force transducers, but the microscale-specific issues mentioned in **Table 1** create many technical and methodological challenges for proposing a standard reference for forces below the newton level (84). At this scale, microbalances are seen as a solution to perform calibration in a more traceable way (16, 85–87). They generally have a plate on which the force is applied vertically at its center. In a compensated mode, the height of the plate is tightly controlled in closed loop, measured by a position sensor and actuated by an electromagnetic or electrostatic actuator. With that compensation, the contact point height remains precisely at a defined position, simplifying the calibration because only the force-sensing body of the tested sensor is deformed during the process. This method is particularly widespread and has succeeded in obtaining an extremely low overall uncertainty, with a ratio of 2 ppm for a weight of 5 g at the US National Institute of Standards and Technology (75, 88), and allowed the redefinition of the kilogram with an uncertainty of 0.01 ppm (89).

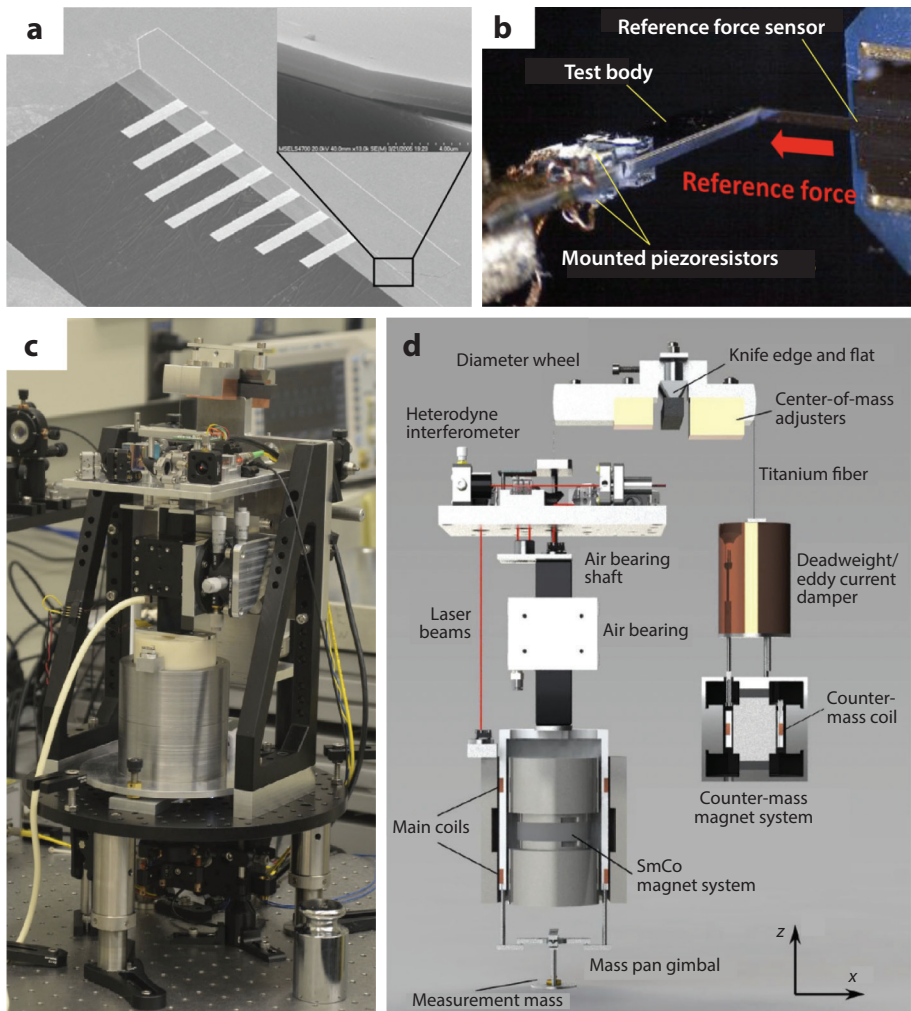


Figure 5

(*a*) Calibration of microforce sensors using calibrated cantilevers. Panel adapted with permission from Reference 74; copyright 2006 IOP Publishing, all rights reserved. (*b*) Calibration of microforce sensors using a calibrated force sensor as a reference. Panel adapted from Reference 24 (CC BY 4.0). (*c,d*) Picture (panel *c*) and component schematic (panel *d*) of a compensated microbalance for traceable measurements. Panels adapted from Reference 75 (CC BY 3.0).

By taking into account practical issues such as zero-point stability, angle deviation between the reference and measurement, and environmental changes, Marti et al. (90) were able to calibrate a capacitive force sensor of 200- μ N, 2-mN, and 20-mN ranges. A compensated balance was used at several national metrology institutes, such as the German Physikalisch-Technische Bundesanstalt (PTB) and the Swiss Federal Institute of Metrology (METAS), which used the same measurement procedure with a precise external micropositioning stage that generated the relative motion between the force-sensing body and substrate. Adding up all the influence factors resulted in an uncertainty of 0.27% (91).

Calibration using another microforce sensor as a reference is practical to set up and provides a versatile way to calibrate sensors, but the uncertainty is at least several percentage points because

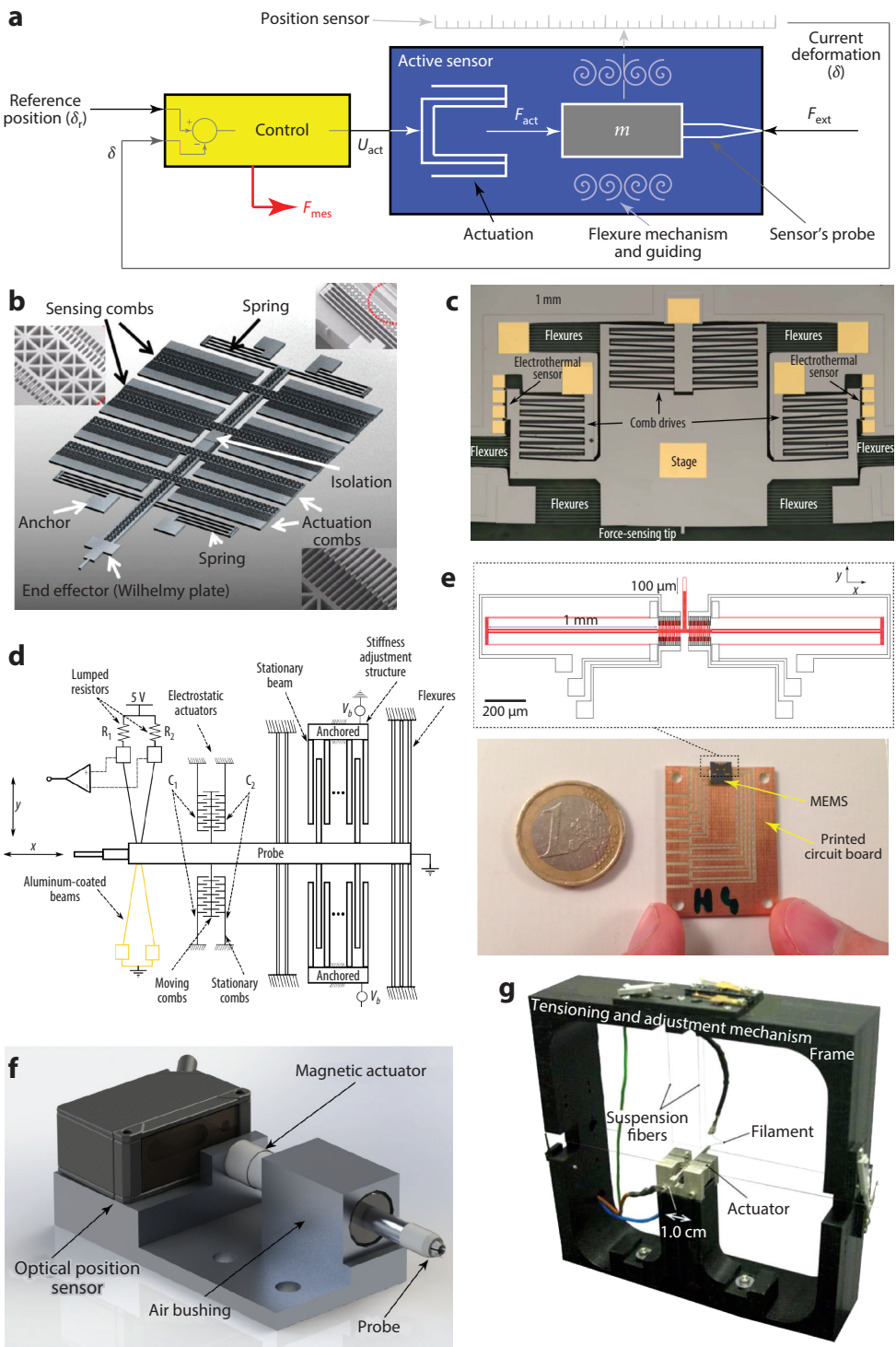
of the errors propagated from the transfer reference used. As described by Yang et al. (1), research on traceable calibration processes is being conducted by different national metrology institutes; most studies are based on microbalances, and results so far demonstrate reduced uncertainties in studies using comparative measurement (90).

5. ACTIVE MICROFORCE SENSING

The most common force-sensing technique is based on the measurement of the deformation δ of the force-sensing body, whose stiffness k is known. Thus, the force measured in static mode is $k \times \delta$. Such sensors are called passive sensors (4, 5). The alternative active sensors' working principle is based on force balancing between an unknown force and a known quantity (92). These sensors integrate an actuator controlled in closed loop to generate a force F_{act} that keeps the position of the sensing probe, and therefore the deformation of the sensing body, at a reference value δ_r when an external force F_{ext} is applied to it (**Figure 6a**). F_{ext} is the force to be measured. It is deduced from the control signal U_{act} to within a constant factor that is a function of the actuator's properties. The performance of passive sensors in terms of resolution, measuring range, and bandwidth depends on their mechanical properties. The stiffness is one of the most influential parameters—the lower the stiffness, the higher the resolution, but at the cost of a lower measuring range and bandwidth. Typically, there is a trade-off between the resolution and measuring range on the one hand and the resolution and frequency bandwidth on the other. With active sensing, these trade-offs can be overcome (40).

The basic architecture of active sensors includes an actuator, a compliant mechanism, a position sensor, and a control algorithm for the probe's position regulation. When using microelectromechanical system (MEMS) technology, the electrostatic comb drive actuator is used most often (37, 38, 40, 92, 93). With a standard comb drive structure, the generated driving force is proportional to the square of the electric input voltage (37, 38, 93). To deal with this nonlinearity, some solutions have linearized this nonlinear characteristic (96) or instrumented the actuator with a square root input voltage (93). The electrical nonlinearity can also be removed with differential comb drive actuation (40, 92). For the compliant mechanism, the mechanical linearity (force/displacement relation) and the stiffness ratio (stiffness in the orthogonal direction of the measurement divided by the stiffness in the direction of the measurement) are the two main parameters that are considered for the selection of the appropriate architecture (97). For instance, with doubly clamped flexures, a mechanical nonlinearity appears for large displacements, leading to a so-called cubic stiffness. This nonlinearity can be handled with appropriate linear parameter-varying (LPV) controllers (98, 99). To measure the position of the probe in active sensors, several principles have been used, including those based on capacitive (37, 38), electrothermal (93), piezoresistive (40), vision (92), and laser (39, 95) technologies. The control strategy used for the sensor's probe regulation is often designed to be as simple as possible. Reported techniques have been based on integral control (93), internal model control and resonant control (40), proportional–integral–derivative (PID) control (38, 92), and state feedback control (95). Most of the time, the main issues in control are related to the precision in keeping the probe at a reference value, the damping of the oscillations, and the stability margin.

Koo & Ferreira (38) designed and fabricated a MEMS force sensor based on a standard comb drive actuator with an integrated capacitive sensor (**Figure 6b**). This sensor is able to measure forces up to 300 μN with a resolution of 25 nN. It has been used in closed loop to measure the surface tension of various liquids. Moore et al. (93) used the sensor for stiffness characterization of microcantilevers (**Figure 6c**). Maroufi et al. (40) incorporated a mechanism to adjust the sensor's stiffness via an electrical voltage (**Figure 6d**). The mechanism is based on an electrostatic actuator that generates a restoring force characterized by negative stiffness. This capability is useful when



(Caption appears on following page)

Figure 6 (Figure appears on preceding page)

Active force sensors. (a) Schematic view of an active force sensor working principle. (b) MEMS active force sensor with a comb drive actuator and folded flexures used for measuring the surface tension of various liquids. Panel adapted with permission from Reference 38; copyright 2014 Elsevier. (c) Active sensor used for stiffness characterization of microcantilevers. Panel adapted with permission from Reference 93; copyright 2015 IEEE. (d) MEMS active force sensor with an adjustable stiffness mechanism. Panel adapted with permission from Reference 40; copyright 2018 Elsevier. (e) MEMS active force sensor with a linear electromechanical characteristic (probe displacement/actuation voltage). Panel adapted with permission from Reference 94; copyright 2018 IEEE. (f) Active force sensor based on nil-stiffness guidance and electromagnetic actuation. Panel adapted with permission from Reference 95; copyright 2020 IEEE. (g) Active force sensor used for haptics applications. Panel adapted with permission from Reference 39; copyright 2015 IEEE. Abbreviation: MEMS, microelectromechanical system.

it comes to adapting the rigidity of the sensor to that of the object to be characterized. Nastro et al. (9) integrated a dual actuator assisted by a position feedback mechanism in a MEMS active force sensor. This original double-actuator mechanism enables the sensor's sensitivity to be adjusted electrically, independent of the working position and the stiffness of the sensors' internal moving mechanical structure. Cailliez et al. (92) incorporated differential comb drive actuation and a folded-type flexure into the sensor (**Figure 6e**), making it a unique active MEMS sensor with a linear electromechanical characteristic (probe displacement/actuation voltage) in the literature.

Cailliez et al. (95) designed and fabricated an original active force sensor based on nil-stiffness guidance and electromagnetic actuation and experimentally tested it for the measurement of a magnetic force (**Figure 6f**). This sensor is suitable for measuring forces from the millinewton to the newton range. Another original active force sensor based on a comb drive actuator was reported by Ousaid et al. (39). This sensor (**Figure 6g**) integrates fibers as a compliant mechanism, which allows the measurement of forces at very low frequencies (cutoff frequency around 10 Hz in open loop). The distinctive aspect of this sensor is that it has been coupled with a haptic interface that has allowed numerous applications, such as feeling capillary forces (39), teleoperation with force feeling for injection in biological samples (100), and feeling what an insect feels like (101). Last but not least, Piat et al. (53) and Amokrane et al. (102) reported original passive nanoforce sensors based on diamagnetic levitation. These sensors are particularly suitable for measuring nanonewton forces at very low frequencies (a few hertz). Amokrane et al. (102) presented a passive version of the sensor and are planning an active version in future works.

Active sensing is still an open research area. Research works have demonstrated several proofs of concept where actuation and control play a fundamental role in force-sensing performance (e.g., resolution, sensitivity, measurement range, and bandwidth). The performance can be tuned and modified online during the measurement process.

6. MICROROBOTIC MICROFORCE-SENSING SYSTEMS AND APPLICATIONS

This section focuses on existing scientific instruments for microforce sensing using microrobotics. It discusses the benefits and challenges of both tethered and untethered systems, providing examples of each, and examines systems with embedded microforce-sensing capabilities.

6.1. Untethered Systems

Untethered systems have the benefit of extra versatility and mobility in the workspace, since they are not bound to any larger subsystem (power source, actuation module, etc.). Moreover, they are capable of reaching small areas and are even usable for *in vivo* applications, where the size constraints are extremely tight and remote untethered operation is likely the only viable option. On

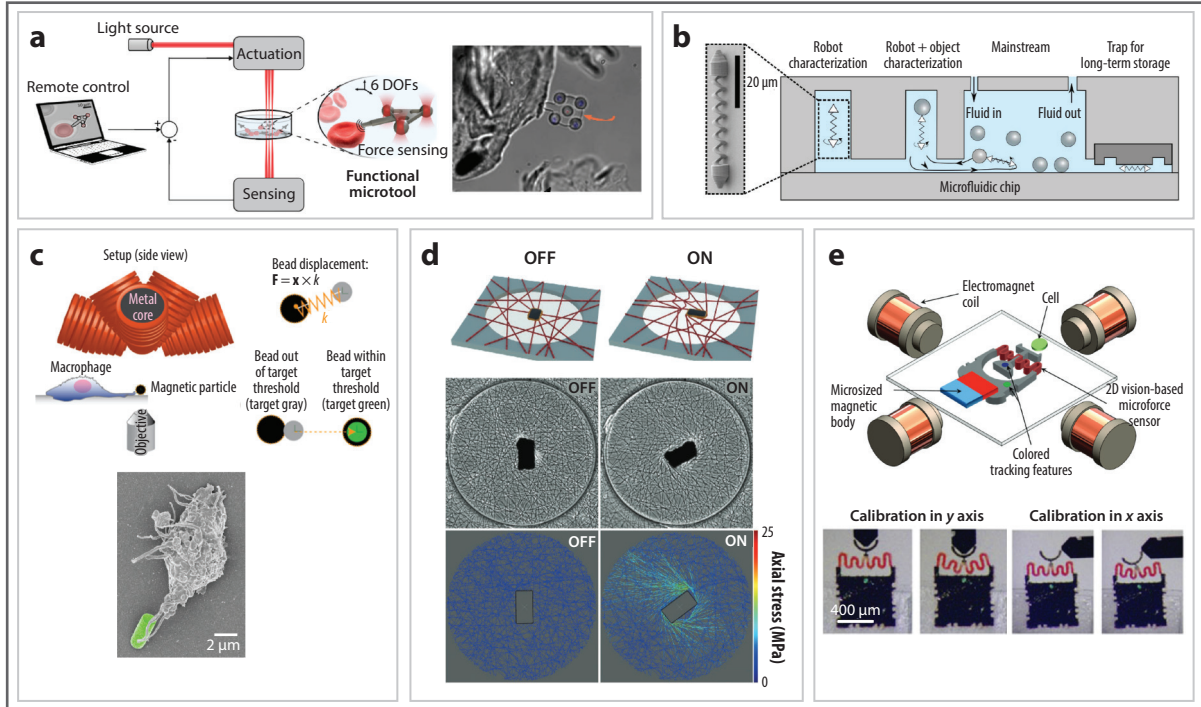


Figure 7

Untethered microrobotic systems with force-sensing capabilities. (a) Force feedback based on computer vision measurement of an optically driven microrobot for interactive biomanipulation. Panel adapted with permission from Reference 28; copyright 2023 Elsevier. (b) Helical microrobot used for force sensing inside a microfluidic chip. Panel adapted with permission from Reference 50; copyright 2017 Elsevier. (c) Force and torque sensing based on magnetic actuation and vision feedback for biological cell–robot interaction. Panel adapted with permission from Reference 27; copyright 2017 The American Association for the Advancement of Science. (d) Rotation of a microactuator resulting in spatially heterogeneous forces in the network, with tensile or compressive mechanical stresses dependent on the fiber orientation and local connectivity. Panel adapted from Reference 103 (CC BY 4.0). (e) 2D vision-based microforce sensing with colored fiducials for biological or synthetic object characterization. Panel adapted with permission from Reference 29; copyright 2018 IEEE. Abbreviation: DOF, degree of freedom.

the other hand, because they have a limited footprint and need to have all of their capabilities onboard (sensing, power, actuation, etc.), the types of force sensors that can be used in such systems are severely limited. For instance, force sensors that require some sort of circuitry for their measurements are most likely tethered, since there is not enough onboard space for the electrical circuit, and the measured forces somehow need to be transmitted to the operator. Therefore, most untethered microforce-sensing systems usually rely on some type of optical or field-driven actuation and sensing.

For example, Gerena & Haliyo (28) utilized optical traps to actuate microrobots and to receive force feedback. The optical traps are able to move the beads shown in Figure 7a and consequently the microrobot itself. As the microrobot pushes against a foreign object, a measurable change in displacement in the optical trap occurs, enabling the measurement of forces and torques applied to or by the microrobot. The use of optical traps (also called optical tweezers) is particularly significant when dealing with single-molecule applications, as the maximum force and trap stiffness are directly proportional to the laser power of the system. Furthermore, there are other, less complex force-sensing alternatives if piconewton resolution is not needed.

Recently, the use of vision-based force sensors, along with an untethered microrobotic platform, has gained some traction. This type of microforce sensor is extremely simple—it requires only a compliant structure of known stiffness and a method to track its deflection (usually via a camera feed), which allows a very small sensing footprint. Thus, the microrobot is able to provide the actuation and force application, while a vision system tracks the deflections and computes the forces. Barbot et al. (50) used an untethered helical magnetic microrobot to measure piconewton-level forces inside a microfluidic chip through a vision-based sensing technique. The microrobot's actuation (the input magnetic field strength and its resultant motion) was linked to the exerted force, obtained by a series of simulations and calibrations (**Figure 7b**). Differences in the observed motion then allowed the computation of the exerted forces inside the microfluidic chip.

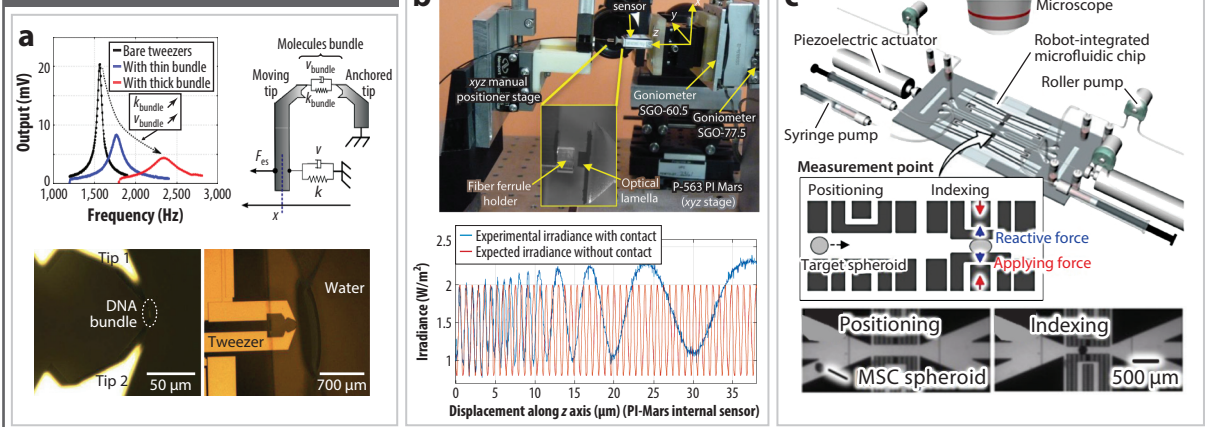
Similarly, Schuerle et al. (27) utilized magnetic particles to measure rotational or translational forces applied by a macrophage as it pulls a “prey” material (**Figure 7c**). In this case, a vision system tracks the position of the magnetic particle in real time, and as the macrophage pulls it, a controller enables a magnetic actuation system to counteract the macrophage forces and keep the particle in place. Analyzing the needed input to the coil system allows the force applied by the macrophage to be computed. Uslu et al. (103) utilized untethered magnetic microactuators to deform fibrous extracellular matrices and apply desired forces (**Figure 7d**). This work used a digital twin experiment re-created using a computer vision algorithm, along with an accurate finite element model, to test virtual mechanical actuation schemes. This is of great benefit to the tissue engineering and mechanobiology fields, as studies of how applied forces affect cells and tissues are crucial.

Guix et al. (29) utilized a wireless magnetic microrobot with a vision-based force sensor to obtain real-time micronewton-level force sensing (**Figure 7e**). This was done by utilizing a compliant spring-like structure, of precalibrated stiffness, and using a computer vision algorithm to measure its deflection, allowing for force computation via Hooke's law. A similar force-sensing system has also been employed in tethered systems (13, 104) by utilizing a micropositioning stage instead of magnetic actuation, providing more spatial accuracy and enabling cooperative applications with force sensing, which are especially useful in fields of mechanical characterization of biological media and micromanipulation/microassembly. As previously mentioned, the use of vision-based force sensors provides a promising avenue for the next generation of force-sensing microrobotic systems, especially untethered systems, in which sensor footprint considerations are extremely important. With the development of higher-speed cameras, vision-based force sensors become even more desirable, since higher resolutions at higher speeds are possible. Moreover, researchers are starting to investigate the use of discrete-time cameras as a possible solution to further improve sensing speed and resolution.

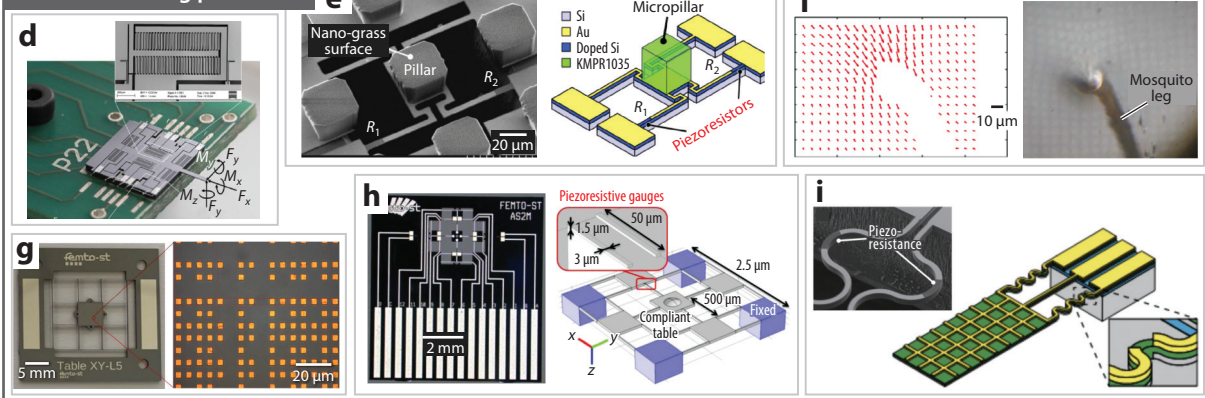
6.2. Tethered Systems

In tethered systems, the sensing instrument is usually attached to a micro/nanopositioning robotic system, allowing for several DOFs and high motion resolution. In the generic configuration shown in **Figure 1**, either the samples' substrate or the tip of the robot (the robot's tool) can be instrumented. Several studies have highlighted the importance of placing the sensor body as close as possible to the contacts where the measurement takes place (3, 105). **Figure 8a–c** introduces several examples. Lafitte et al. (106, 107) (**Figure 8a**) showed that implementing the state feedback of instrumented silicon nanotweezers enables the reduction of the resonant frequency of the system, improving the sensitivity of mechanical stiffness measurements and the biosensing of DNA molecules. Bettahar et al. (108) (**Figure 8b**) introduced a system combining a compliant structure with a laser so that optical Fabry–Perot interference occurs between them. High-resolution position measurement is achieved when a relative motion without contact happens based on

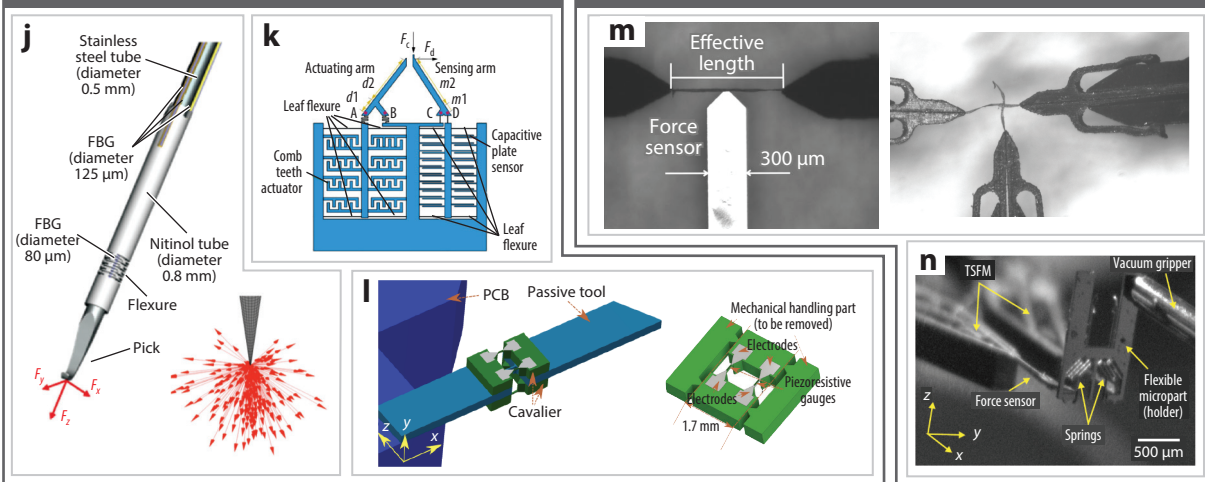
Real-time force control



Multiaxis sensing platforms



Multiaxis instrumented robotic tools



(Caption appears on following page)

Figure 8 (Figure appears on preceding page)

Tethered microrobotic systems with force-sensing capabilities. (a–c) Real time force/position measurement. (a) Instrumented nanotweezers for mechanical characterization of DNA (106, 107). Panel adapted with permission from Reference 106; copyright 2013 IEEE. (b) Force–position sensing based on a photorobotic approach. Panel adapted from Reference 108. (c) Force-deformation compression inside of a robot-integrated microfluidic chip. Panel adapted with permission from Reference 109; copyright 2019 IEEE. (d–i) Multiaxis force- and/or torque-sensing platforms. (d) Six-axis MEMS force–torque sensor (capacitive). Panel adapted with permission from Reference 7; copyright 2009 IEEE. (e) Two-axis MEMS-based force sensor (piezoresistive gauge). Panel adapted with permission from Reference 110; copyright 2015 Elsevier. (f) Three-axis force sensor (vision). Panel adapted with permission from Reference 15; copyright 2019 IEEE. (g) Three-axis microforce- and torque-sensing platform (vision). Panel adapted with permission from Reference 14; copyright 2021 IEEE. (h) Multiaxis microforce and torque sensor (piezoresistive gauges). Panel adapted from Reference 111 with permission from Inderscience Enterprises Limited; permission conveyed through Copyright Clearance Center, Inc. (i) MEMS two-axis force plate array. Panel adapted with permission from Reference 26; copyright 2006 IOP Publishing, all rights reserved. (j–l) Robotic tools integrating multiaxis force-sensing capabilities. (j) Three-axis force-sensing instrument with integrated FBG. Panel adapted with permission from Reference 20; copyright 2014 IEEE. (k) Dual-axis force-sensing gripper for grasping biocellulose. Panel adapted from Reference 112 with permission from the American Society of Mechanical Engineers; permission conveyed through Copyright Clearance Center, Inc. (l) Two-axis piezoresistive force-sensing tool for microgripping. Panel adapted with permission from Reference 24 (CC BY 4.0). (m,n) Robotic tasks based on multiaxis force control. (m) Shear-mode bonding force and flexibility test of single pulp fibers (113, 114). Panel adapted from Reference 114 with permission from John Wiley and Sons; permission conveyed through Copyright Clearance Center, Inc. (n) Hybrid force–position control for automated microassembly (62, 115–117). Panel adapted from Reference 117. Abbreviations: FBG, fiber Bragg grating; MEMS, microelectromechanical system; MSC, mesenchymal stem cell; PCB, printed circuit board; TSFM, two-smart-fingers microgripper.

sine optical measurements having a constant periodicity. Once a contact happens, the compliant structure deforms and the periodicity of the optical signal increases, enabling one to estimate the force applied and resulting in a high-resolution position–force measurement. Sakuma et al. (109) (**Figure 8c**) integrated a compliant structure inside of a microfluidic chip; through the use of a piezoactuator and vision feedback, this structure induces a force-deformation compression of single-cell spheroids inside the microfluidic chip. In addition, control-related works aimed at mastering the grasping force for micromanipulation tasks have been published (118–120).

While the abovementioned works have dealt with the measurement of microforces in one direction, several studies have naturally focused on the development of sensors capable of measuring in several directions or of performing force–torque sensing or force–position sensing together. **Figure 8d–i** highlights examples of multiaxis sensing platforms. The main works in the literature are based on microfabricated compliant structures combined with a six-axis MEMS force–torque sensor (using capacitive sensing) (7) (**Figure 8d**); a two-axis MEMS-based force sensor (piezoresistive gauge) to study capillary forces by measuring the interaction forces during the sliding of a droplet on a micropillar array (110) (**Figure 8e**); a three-axis force sensor (vision) for detecting insect motion by evaluating the deformation of a grid pattern inscribed in a flexible hydrogel sheet (15) (**Figure 8f**); a three-axis microforce- and torque-sensing platform (vision) by tracking a periodic pattern inscribed on the platform, enabling Fourier-based transform for accurate microassembly (14) (**Figure 8g**); a multiaxis microforce and torque sensor (piezoresistive gauges) for measuring friction forces where it is necessary to measure the preload as well as the lateral force (111) (**Figure 8h**); and a MEMS two-axis force plate array to measure the ground reaction forces during the running motion of an ant (26) (**Figure 8i**). Other works have also developed robotic tools integrating multiaxis force-sensing capabilities. For them, the integrability of the sensing principle is a key challenge. **Figure 8j–l** provides several complementary examples: a three-axis force-sensing instrument with integrated fiber Bragg grating for retinal microsurgery (20) (**Figure 8j**), whose principle can also be used for drug injection (121) or neurosurgery (122); a dual-axis force-sensing MEMS gripper for grasping biocellulose (112) (**Figure 8k**); and a two-axis piezoresistive force-sensing tool for micrograsping microassembly (24) or control of gluing tasks (123) (**Figure 8l**).

The majority of these instrumented platforms and instrumented robotic tools open the way to applications requiring simultaneous measurement in several directions or simultaneous measurement of force and position. Beyond the question of how to integrate all the devices together, understanding the dynamic response of the systems and successfully controlling them together become key challenges. **Figure 8m,n** introduces several examples of such systems. Saketi (113) and Grigoray et al. (114) developed a system to investigate the shear-mode bonding force measurement process and photocontrol of mechanical properties through a flexibility test of single pulp fibers (**Figure 8m**). The automated microassembly of compliant optical components using an instrumented microgripper and hybrid force/position control was demonstrated by Komati and colleagues (115–117) (**Figure 8n**). Accurate tasks are made possible by such multiaxis force-sensing capabilities because they enable the implementation of robotic strategies that can be adapted to the presence of adhesion forces (62) to simultaneously control force and position (or force and vision) for tasks such as guidance, insertion, or alignment of components (124–127).

Researchers are also working on enabling robots to adapt to changes in the stiffness of the working environment, such as for mini-invasive surgery tools. Li et al. (121) demonstrated that robot-assisted ophthalmic surgery can be significantly improved by 3D microforce perception that helps the surgeon to align and then guide the tool. There is also interest in applications such as elasticity sensing based on different tactile properties (128), to assist the microinjection of both adherent and suspended cells by guiding the robot (2, 129, 130) and for the purpose of mechanical characterization where multiaxis sensing and control enable the study of certain influential parameters. Govilas et al. (131) demonstrated that small angular errors during diametral compression tests of single plant fibers resulted in large errors in the estimate of their Young modulus (an angular error of 1° induces a 35% error) based on multiaxis force–position sensing (132). For accurate control of micropositioning robots, they proposed a robotic strategy to enable control of angles smaller than 0.1°.

All of these works paved the way for the creation of tethered microrobotic systems for microforce sensing using different measurement principles, and have also enabled the use of these systems to achieve complex tasks by measuring local information such as contact forces. Ongoing progress in microfabrication techniques, notably 3D printing, and the improvement of interfaces enabling dynamic and synchronized control of several dynamic systems are key reasons to believe that these types of microrobotic systems for microforce sensing will develop significantly in the coming years.

7. CONCLUSIONS

The robotics and automation tools presented in this article are intended to help researchers develop experimental devices capable of performing efficient microforce sensing, taking advantage of intrinsic capabilities of microrobotic systems such as versatility, high dynamics, and multi-DOF motion capabilities. This article aimed to present for the first time an overview of force-sensing systems by considering the robot, sensor, and control architecture as a whole.

A key feature of microrobotic systems for microforce sensing relates to traceability. In the coming years, these systems are expected to provide new standards and measurement protocols that can be easily applied in both research and industry to guarantee the trueness of the measured force, which is still an open challenge.

Most microrobotic systems used for microforce sensing are commercially available today, but they still present major limitations in terms of the accessibility of sensor tips in hard-to-reach areas and the measurement of distributed forces. Many research teams are investigating new robotic principles that are expected to overcome several of these limitations, by increasing the

miniaturization of robots' end effectors and/or by designing soft robots or robots able to perform continuous deformations. These works will open avenues for different ways to control or measure forces. For instance, most works today are based on measuring a force at a contact point (or a small surface). Future works might be oriented to the measurement of distributed forces that could be made possible by smart materials and/or novel fabrication methods, such as 3D/4D printing.

Last but not least, force-based microrobotic systems under development enable researchers to study different experimental protocols that provide a rich set of data, notably on force, position, deformation, temperature, and so on. The sharing and analysis of these data should enable the exchange of best practices and the standardization of experimental devices and protocols. These data will also be important for the use of learning-based methods, which are useful not only in guiding designs but also for using experimental systems in an optimal way to achieve efficient microforce sensing based on microrobotics.

DISCLOSURE STATEMENT

The authors are not aware of any affiliations, memberships, funding, or financial holdings that might be perceived as affecting the objectivity of this review.

ACKNOWLEDGMENTS

This work was supported by the National Science Foundation (Information and Intelligent Systems award 1763689 and Civil, Mechanical, and Manufacturing Innovation award 2018570), the FACE Foundation, the Chateaubriand STEM Fellowship program, the DYNABOT Project (contract ANR-21-CE10-0016), the Bourgogne-Franche-Comté Région, and the Engineering and Innovation Through Physical Sciences, High Technologies, and Cross-Disciplinary Research (EIPHI) Graduate School (contract ANR-17-EURE-0002).

LITERATURE CITED

1. Yang Y, Zhao M, Yinguo H, Zhang H, Guo N, Zheng Y. 2022. Micro-force sensing techniques and traceable reference forces: a review. *Measur. Sci. Technol.* 33(11):114010
2. Wei Y, Xu Q. 2019. A survey of force-assisted robotic cell microinjection technologies. *IEEE Trans. Autom. Sci. Eng.* 16(2):931–45
3. Zang H, Zhang X, Zhu B, Fatikow S. 2019. Recent advances in non-contact force sensors used for micro/nano manipulation. *Sens. Actuators A* 296:155–77
4. Wei Y, Xu Q. 2015. An overview of micro-force sensing techniques. *Sens. Actuators A* 234:359–74
5. Boudaoud M, Régnier S. 2014. An overview on gripping force measurement at the micro and nano-scales using two-fingered microrobotic systems. *Int. J. Adv. Robot. Syst.* 11(3). <https://doi.org/10.5772/57571>
6. Muntwyler S, Beyeler F, Nelson BJ. 2009. Three-axis micro-force sensor with sub-micro-Newton measurement uncertainty and tunable force range. *J. Micromech. Microeng.* 20(2):25011
7. Beyeler F, Muntwyler S, Nelson BJ. 2009. A six-axis MEMS force-torque sensor with micro-Newton and nano-Newtonmeter resolution. *J. Microelectromech. Syst.* 18(2):433–41
8. Kim K, Cheng J, Liu Q, Wu XY, Sun Y. 2010. Investigation of mechanical properties of soft hydrogel microcapsules in relation to protein delivery using a MEMS force sensor. *J. Biomed. Mater. Res. A* 92A(1):103–13
9. Nastro A, Ferrari M, Ferrari V. 2020. Double-actuator position-feedback mechanism for adjustable sensitivity in electrostatic-capacitive MEMS force sensors. *Sens. Actuators A* 312:112127
10. Stange A, Imboden M, Javor J, Barrett LK, Bishop DJ. 2019. Building a Casimir metrology platform with a commercial MEMS sensor. *Microyst. Nanoeng.* 5(1):14
11. Gao W, Liu C, Han X, Zhao L, Lin Q, et al. 2023. A high-resolution MEMS capacitive force sensor with bionic swallow comb arrays for ultralow multiphysics measurement. *IEEE Trans. Ind. Electron.* 70(7):7467–77

12. Chu HK, Mills JK, Cleghorn WL. 2007. Design of a high sensitivity capacitive force sensor. In *2007 7th IEEE Conference on Nanotechnology*, pp. 29–33. Piscataway, NJ: IEEE
13. Adam G, Chidambaram S, Reddy SS, Ramani K, Cappelleri DJ. 2021. Towards a comprehensive and robust micromanipulation system with force-sensing and VR capabilities. *Micromachines* 12(7):784
14. Tiwari B, Blot M, Laurent GJ, Agnus J, Sandoz P, et al. 2021. A high range-to-resolution multiaxis μ force and torque sensing platform. *IEEE/ASME Trans. Mech.* 26(4):1837–45
15. Suzuki M, Takahashi T, Aoyagi S. 2019. A distributed 3D force sensor for detecting insect motion by optically evaluating deformation of microscale grid pattern inscribed on a flexible hydrogel sheet. In *2019 20th International Conference on Solid-State Sensors, Actuators and Microsystems and Eurosensors XXXIII*, pp. 2504–7. Piscataway, NJ: IEEE
16. Guo X, Zhang Y, Cao M, Shu Q, Knoll A, et al. 2023. Mechanical force characterization of living cells based on needle deformation. *Adv. Mater. Interfaces* 10(20):2300293
17. Guelpa V, Laurent GJ, Sandoz P, Clévy C. 2015. Vision-based microforce measurement with a large range-to-resolution ratio using a twin-scale pattern. *IEEE/ASME Trans. Mechatron.* 20(6):3148–56
18. Zou M, Liao C, Liu S, Xiong C, Zhao C, et al. 2021. Fiber-tip polymer clamped-beam probe for high-sensitivity nanoforce measurements. *Light Sci. Appl.* 10(1):171
19. Tang Y, Liu H, Pan J, Zhang Z, Xu Y, et al. 2021. Optical micro/nanofiber-enabled compact tactile sensor for hardness discrimination. *ACS Appl. Mater. Interfaces* 13(3):4560–66
20. He X, Handa J, Gehlbach P, Taylor R, Iordachita I. 2014. A submillimetric 3-DOF force sensing instrument with integrated fiber Bragg grating for retinal microsurgery. *IEEE Trans. Biomed. Eng.* 61(2):522–34
21. Wei Y, Xu Q. 2017. Design of a PVDF-MFC force sensor for robot-assisted single cell microinjection. *IEEE Sens. J.* 17(13):3975–82
22. Behrens I, Doering L, Peiner E. 2003. Piezoresistive cantilever as portable micro force calibration standard. *J. Micromech. Microeng.* 13(4):S171–77
23. Qu J, Wu Q, Clancy T, Fan Q, Wang X, Liu X. 2020. 3D-printed strain-gauge micro force sensors. *IEEE Sens. J.* 20(13):6971–78
24. Tiwari B, Billot M, Clévy C, Agnus J, Piat E, Lutz P. 2021. A two-axis piezoresistive force sensing tool for microgripping. *Sensors* 21(18):6059
25. Komati B, Clévy C, Rakotondrabe M, Lutz P. 2014. Dynamic force/position modeling of a one-DOF smart piezoelectric micro-finger with sensorized end-effector. In *2014 IEEE/ASME International Conference on Advanced Intelligent Mechatronics*, pp. 1474–79. Piscataway, NJ: IEEE
26. Takahashi H, Thanh-Vinh N, Jung UG, Matsumoto K, Shimoyama I. 2014. MEMS two-axis force plate array used to measure the ground reaction forces during the running motion of an ant. *J. Micromech. Microeng.* 24(6):65014
27. Schuerle S, Vizcarra IA, Moeller J, Sakar MS, Özkal B, et al. 2017. Robotically controlled microprey to resolve initial attack modes preceding phagocytosis. *Sci. Robot.* 2(2):eaah6094
28. Gerena E, Haliyo S. 2023. 3D force-feedback optical tweezers for experimental biology. In *Robotics for Cell Manipulation and Characterization*, ed. C Dai, G Shan, Y Sun, pp. 145–72. San Diego, CA: Academic
29. Guix M, Wang J, An Z, Adam G, Cappelleri DJ. 2018. Real-time force-feedback micromanipulation using mobile microrobots with colored fiducials. *IEEE Robot. Autom. Lett.* 3(4):3591–97
30. FemtoTools. 2023. Home page. *FemtoTools*. <https://www.femtotools.com>
31. THK Precis. 2023. Home page. *THK Precision*. <https://www.thkprecision.co.jp>
32. CLA. 2023. Home page. *CLA*. <https://www.cla.ch>
33. Transducer Tech. 2023. Home page. *Transducer Techniques*. <https://www.transducertechniques.com>
34. Futek. 2023. Home page. *Futek*. <https://www.futek.com>
35. TEL. 2023. Home page. *TEI*. <https://www.tei.fr>
36. Moore SI, Coskun MB, Alan T, Neild A, Moheimani SOR. 2015. Feedback-controlled MEMS force sensor for characterization of microcantilevers. *J. Microelectromech. Syst.* 24(4):1092–101
37. Zhang L, Dong J. 2012. Design, fabrication, and testing of a SOI-MEMS-based active microprobe for potential cellular force sensing applications. *Adv. Mech. Eng.* 4:785798
38. Koo B, Ferreira PM. 2014. An active MEMS probe for fine position and force measurements. *Precis. Eng.* 38(4):738–48

39. Ousaid AM, Haliyo DS, Régnier S, Hayward V. 2015. A stable and transparent microscale force feedback teleoperation system. *IEEE/ASME Trans. Mechatron.* 20(5):2593–603
40. Maroufi M, Alemansour H, Bulut Coskun M, Moheimani SOR. 2018. An adjustable-stiffness MEMS force sensor: design, characterization, and control. *Mechatronics* 56:198–210
41. Barile G, Ferri G, Parente FR, Stornelli V, Sisinni E, et al. 2018. A CMOS full-range linear integrated interface for differential capacitive sensor readout. *Sens. Actuators A* 281:130–40
42. Cellini F, Khapli S, Peterson SD, Porfiri M. 2014. Mechanochromic polyurethane strain sensor. *Appl. Phys. Lett.* 105(6):061907
43. Ștefanescu DM, Farcașiu AT, Toader A. 2012. Strain gauge force transducer and virtual instrumentation used in a measurement system for retention forces of palatal plates or removable dentures. *IEEE Sens. J.* 12(10):2968–73
44. Gnerlich M, Perry SF, Tatic-Lucic S. 2012. A submersible piezoresistive MEMS lateral force sensor for a diagnostic biomechanics platform. *Sens. Actuators A* 188:111–19
45. Xie Y, Zhou Y, Lin Y, Wang L, Xi W. 2016. Development of a microforce sensor and its array platform for robotic cell microinjection force measurement. *Sensors* 16(4):483
46. Hasegawa Y, Shikida M, Ogura D, Suzuki Y, Sato K. 2008. Fabrication of a wearable fabric tactile sensor produced by artificial hollow fiber. *J. Micromech. Microeng.* 18(8):085014
47. De Maria G, Natale C, Pirozzi S. 2012. Force/tactile sensor for robotic applications. *Sens. Actuators A* 175:60–72
48. Yussof H, Ohka M, Kobayashi H, Takata J, Yamano M, Nasu Y. 2007. Development of an optical three-axis tactile sensor for object handing tasks in humanoid robot navigation system. In *Autonomous Robots and Agents*, ed. SC Mukhopadhyay, GS Gupta, pp. 43–51. Berlin: Springer
49. Puangmali P, Althoefer K, Seneviratne LD, Murphy D, Dasgupta P. 2008. State-of-the-art in force and tactile sensing for minimally invasive surgery. *IEEE Sens. J.* 8(4):371–80
50. Barbot A, Decanini D, Hwang G. 2017. Helical microrobot for force sensing inside microfluidic chip. *Sens. Actuators A* 266:258–72
51. Borovic B, Liu AQ, Popa D, Cai H, Lewis FL. 2005. Open-loop versus closed-loop control of MEMS devices: choices and issues. *J. Micromech. Microeng.* 15(10):1917
52. Devasia S, Eleftheriou E, Moheimani SOR. 2007. A survey of control issues in nanopositioning. *IEEE Trans. Control Syst. Technol.* 15(5):802–23
53. Piat E, Abadie J, Oster S. 2012. Nanoforce estimation based on Kalman filtering and applied to a force sensor using diamagnetic levitation. *Sens. Actuators A* 179:223–36
54. Boudaoud M, Haddab Y, Le Gorrec Y. 2013. Modeling and optimal force control of a nonlinear electrostatic microgripper. *IEEE/ASME Trans. Mechatron.* 18(3):1130–39
55. Chen WH, Yang J, Guo L, Li S. 2016. Disturbance-observer-based control and related methods—an overview. *IEEE Trans. Ind. Electron.* 63(2):1083–95
56. Rakotondrabe M, Rabenorosoa K, Agnus J, Chaillet N. 2011. Robust feedforward-feedback control of a nonlinear and oscillating 2-DOF piezocantilever. *IEEE Trans. Autom. Sci. Eng.* 8(3):506–19
57. Tafazzoli A, Pawashe C, Sitti M. 2006. Force-controlled microcontact printing using microassembled particle templates. In *2006 IEEE International Conference on Robotics and Automation*, pp. 263–68. Piscataway, NJ: IEEE
58. Xu Q. 2014. Design and smooth position/force switching control of a miniature gripper for automated microhandling. *IEEE Trans. Ind. Inform.* 10(2):1023–32
59. Singh SK, Popa DO. 1995. An analysis of some fundamental problems in adaptive control of force and impedance behavior: theory and experiments. *IEEE Trans. Robot. Autom.* 11(6):912–21
60. Komati B, Pac M, Ranatunga I, Clévy C, Popa D, Lutz P. 2013. Explicit force control versus impedance control for micromanipulation. In *ASME 2013 International Design Engineering Technical Conference and Computers and Information in Engineering Conference*, Vol. 1, pap. V001T09A018. New York: Am. Soc. Mech. Eng.
61. Xu Q. 2015. Robust impedance control of a compliant microgripper for high-speed position/force regulation. *IEEE Trans. Ind. Electron.* 62(2):1201–9

62. Komati B, Clévy C, Lutz P. 2019. Sliding mode impedance controlled smart fingered microgripper for automated grasp and release tasks at the microscale. In *Precision Assembly in the Digital Age*, ed. S Ratchev, pp. 201–13. Cham, Switz.: Springer
63. Ru C, Liu X, Sun Y, eds. 2016. *Nanopositioning Technologies: Fundamentals and Applications*. Cham, Switz.: Springer
64. Li Z, Li S, Luo X. 2021. An overview of calibration technology of industrial robots. *IEEE/CAA J. Autom. Syst.* 8(1):23–36
65. Lubrano E. 2011. *Calibration of ultra-high-precision robots operating in an unsteady environment*. PhD Thesis, École Polytech. Féd. Lausanne, Lausanne, Switz.
66. Xu Q, Tan KK. 2016. *Advanced Control of Piezoelectric Micro-/Nano-Positioning Systems*. Cham, Switz.: Springer
67. Popa DO, Murthy R, Das AN. 2009. M³-deterministic, multiscale, multirobot platform for microsystems packaging: design and quasi-static precision evaluation. *IEEE Trans. Autom. Sci. Eng.* 6(2):345–61
68. Mattos LS, Caldwell DG. 2009. A fast and precise micropipette positioning system based on continuous camera-robot recalibration and visual servoing. In *2009 IEEE International Conference on Automation Science and Engineering*, pp. 609–14. Piscataway, NJ: IEEE
69. Tan N, Clévy C, Laurent G, Sandoz P, Chaillet N. 2015. Accuracy quantification and improvement of serial micropositioning robots for in-plane motions. *IEEE Trans. Robot.* 31(6):1497–507
70. Cailliez J, Boudaoud M, Régnier S. 2019. Calibration of a class of 3 DOF serial micro robotic systems through SEM vision: application to vertical AFM tip landing. In *2019 International Conference on Manipulation, Automation and Robotics at Small Scales*. Piscataway, NJ: IEEE. <https://doi.org/10.1109/MARSS.2019.8860990>
71. Tan N, Clévy C, Chaillet N. 2015. Calibration of nanopositioning stages. *Micromachines* 6(12):1856–75
72. Bettahar H, Lehmann O, Clévy C, Courjal N, Lutz P. 2022. 6-DoF full robotic calibration based on 1-D interferometric measurements for microscale and nanoscale applications. *IEEE Trans. Autom. Sci. Eng.* 19(1):348–59
73. Peiner F, Doering L, Balke M, Christ A. 2008. Silicon cantilever sensor for micro-/nanoscale dimension and force metrology. *Microsyst. Technol.* 14:441–51
74. Gates RS, Pratt JR. 2006. Prototype cantilevers for SI-traceable nanonewton force calibration. *Meas. Sci. Technol.* 17(10):2852
75. Chao L, Seifert F, Haddad D, Pratt J, Newell D, Schlamming S. 2020. The performance of the KIBB-g1 tabletop Kibble balance at NIST. *Metrologia* 57(3):35014
76. Frühauf J, Gärtner E, Li Z, Doering L, Spichtinger J, Ehret G. 2022. Silicon cantilever for micro/nanoforce and stiffness calibration. *Sensors* 22(16):6253
77. Collinson DW, Sheridan RJ, Palmeri MJ, Brinson LC. 2021. Best practices and recommendations for accurate nanomechanical characterization of heterogeneous polymer systems with atomic force microscopy. *Prog. Polym. Sci.* 119:101420
78. Hopcroft MA, Nix WD, Kenny TW. 2010. What is the Young's modulus of silicon? *J. Microelectromech. Syst.* 19(2):229–38
79. Adam G, Ulliac G, Clévy C, Cappelleri DJ. 2022. Design and characterization of a fully 3D printed vision-based micro-force sensor for microrobotic applications. In *2022 International Conference on Manipulation, Automation and Robotics at Small Scales*. Piscataway, NJ: IEEE. <https://doi.org/10.1109/MARSS55884.2022.9870488>
80. Xiang D. 2019. Capacitive micro-force sensor as a transfer standard for verification and calibration of nanoindentation instruments. In *Micro- and Nanotechnology Sensors, Systems, and Applications XI*, ed. T George, MS Islam, pp. 534–41. Philadelphia: Soc. Ind. Appl. Math.
81. Li Z, Youssefi O, Diller E. 2016. Magnetically-guided in-situ microrobot fabrication. In *2016 IEEE/RSJ International Conference on Intelligent Robots and Systems*, pp. 5131–36. Piscataway, NJ: IEEE
82. Jang J, Panusa G, Boero G, Brugger J. 2022. SU-8 cantilever with integrated pyrolyzed glass-like carbon piezoresistor. *Microsyst. Nanoeng.* 8(1):22
83. Joint Comm. Guides Metrol. (JCGM). 2012. *International vocabulary of metrology – basic and general concepts and associated terms (VIM)*. Doc. JCGM 200:2012, Joint Comm. Guides Metrol. 3rd ed.

84. Kim MS, Pratt JR. 2010. SI traceability: current status and future trends for forces below 10 microNewtons. *Measurement* 43(2):169–82
85. Yafei Q, Yulong Z, Weizhong W. 2015. Development and characterization of three-axis micro-force sensor series. In *10th IEEE International Conference on Nano/Micro Engineered and Molecular Systems*, pp. 103–6. Piscataway, NJ: IEEE
86. Hamdانا G, Wasisto HS, Doering L, Yan C, Zhou L, et al. 2016. Double-meander spring silicon piezoresistive sensors as microforce calibration standards. *Opt. Eng.* 55(9):091409
87. Zhao Y, Wu B, Jia Y, Li Z. 2023. A micro-force measurement torsion pendulum design with dual laser detection. *J. Phys. Conf. Ser.* 2489:12003
88. Pratt JR, Kramar JA, Newell DB, Smith DT. 2005. Review of SI traceable force metrology for instrumented indentation and atomic force microscopy. *Meas. Sci. Technol.* 16(11):2129
89. Robinson IA, Schlamming S. 2016. The watt or Kibble balance: a technique for implementing the new SI definition of the unit of mass. *Metrologia* 53(5):A46–74
90. Marti K, Aeschbacher M, Russi S, Wuethrich C. 2018. Microforce measurements – a new instrument at METAS. *J. Phys. Conf. Ser.* 1065:42024
91. Marti K, Wuethrich C, Aeschbacher M, Russi S, Brand U, Li Z. 2020. Micro-force measurements: a new instrument at METAS. *Meas. Sci. Technol.* 31(7):75007
92. Cailliez J, Boudaoud M, Mohand-Ousaid A, Weill-Duflos A, Haliyo S, Régnier S. 2019. Modeling and experimental characterization of an active MEMS based force sensor. *J. Micro-Bio Robot.* 15:53–64
93. Moore SI, Coskun MB, Alan T, Neild A, Moheimani SOR. 2015. Feedback-controlled MEMS force sensor for characterization of microcantilevers. *J. Microelectromech. Syst.* 24(4):1092–101
94. Cailliez J, Boudaoud M, Mohand-Ousaid A, Weill-Duflos A, Haliyo S, Régnier S. 2018. Modeling and experimental characterization of an active MEMS based force sensor. In *2018 International Conference on Manipulation, Automation and Robotics at Small Scales (MARSS)*. Piscataway, NJ: IEEE. <https://doi.org/10.1109/MARSS.2018.8481177>
95. Cailliez J, Weill-Duflos A, Boudaoud M, Régnier S, Haliyo S. 2020. Design and control of a large-range nil-stiffness electro-magnetic active force sensor. In *2020 IEEE International Conference on Robotics and Automation*, pp. 9244–50. Piscataway, NJ: IEEE
96. Mohammadi A, Fowler AG, Yong YK, Moheimani SOR. 2014. A feedback controlled MEMS nanopositioner for on-chip high-speed AFM. *J. Microelectromech. Syst.* 23(3):610–19
97. Legtenberg R, Groeneveld AW, Elwenspoek M. 1996. Comb-drive actuators for large displacements. *J. Micromech. Microeng.* 6(3):320
98. Boudaoud M, Gaudenzi De Faria M, Le Gorrec Y, Haddab Y, Lutz P. 2014. An output feedback LPV control strategy of a nonlinear electrostatic microgripper through a singular implicit modeling. *Control Eng. Pract.* 28:97–111
99. Boudaoud M, Le Gorrec Y, Haddab Y, Lutz P. 2015. Gain scheduling control of a nonlinear electrostatic microgripper: design by an eigenstructure assignment with an observer-based structure. *IEEE Trans. Control Syst. Technol.* 23(4):1255–67
100. Mohand-Ousaid A, Haliyo S, Régnier S, Hayward V. 2020. High fidelity force feedback facilitates manual injection in biological samples. *IEEE Robot. Autom. Lett.* 5(2):1758–63
101. Ousaid AM, Millet G, Haliyo S, Régnier S, Hayward V. 2014. Feeling what an insect feels. *PLOS ONE* 9(10):e108895
102. Amokrane F, Drouot A, Abadie J, Piat E. 2020. Nanoforce estimation using interval observer: application to force sensor based on diamagnetic levitation. *IFAC-PapersOnLine* 53(2):8638–43
103. Ushu FE, Davidson CD, Mailand E, Bouklas N, Baker BM, Sakar MS. 2021. Engineered extracellular matrices with integrated wireless microactuators to study mechanobiology. *Adv. Mater.* 33(40):2102641
104. Adam G, Ulliac G, Clévy C, Cappelleri DJ. 2023. 3D printed vision-based micro-force sensors for microrobotic applications. *J. Micro-Bio Robot.* 18:15–24
105. Clévy C, Rakotondrabe M, Chaillet N, eds. 2011. *Signal Measurement and Estimation Techniques for Micro and Nanotechnology*. New York: Springer
106. Lafitte N, Haddab Y, Le Gorrec Y, Kumemura M, Jalabert L, et al. 2013. Closed-loop control of silicon nanotweezers for improvement of sensitivity to mechanical stiffness measurement and bio-sensing on

- DNA molecules. In *2013 IEEE/RSJ International Conference on Intelligent Robots and Systems*, pp. 1022–27. Piscataway, NJ: IEEE
107. Lafitte N, Haddab Y, Le Gorrec Y, Guillou H, Kumemura M, et al. 2014. Improvement of silicon nanotweezers sensitivity for mechanical characterization of biomolecules using closed-loop control. *IEEE/ASME Trans. Mechatron.* 20(3):1418–27
 108. Bettahar H, Clévy C, Courjal N, Lutz P. 2020. Force-position photo-robotic approach for the high-accurate micro-assembly of photonic devices. *IEEE Robot. Autom. Lett.* 5(4):6396–402
 109. Sakuma S, Nakahara K, Arai F. 2019. Continuous mechanical indexing of single-cell spheroids using a robot-integrated microfluidic chip. *IEEE Robot. Autom. Lett.* 4(3):2973–80
 110. Thanh-Vinh N, Takahashi H, Matsumoto K, Shimoyama I. 2015. Two-axis MEMS-based force sensor for measuring the interaction forces during the sliding of a droplet on a micropillar array. *Sens. Actuators A* 231:35–43
 111. Billot M, Xu X, Agnus J, Piat E, Stempflé P. 2015. Multi-axis MEMS force sensor for measuring friction components involved in dexterous micromanipulation: design and optimisation. *Int. J. Nanomanuf.* 11(3–4):161–84
 112. Yang S, Xu Q, Nan Z. 2017. Design and development of a dual-axis force sensing MEMS microgripper. *J. Mech. Robot.* 9(6):061011
 113. Saketi P. 2015. *Microrobotic platform with integrated force sensing microgrippers for characterization of fibrous materials: case study on individual paper fibers*. PhD Thesis, Tampere Univ. Technol., Hervanta, Finland
 114. Grigoray O, Wondraczek H, Daus S, Kühnöl K, Latifi SK, et al. 2015. Photocontrol of mechanical properties of pulp fibers and fiber-to-fiber bonds via self-assembled polysaccharide derivatives. *Macromol. Mater. Eng.* 300(3):277–82
 115. Komati B, Rabenorosoa K, Clévy C, Lutz P. 2013. Automated guiding task of a flexible micropart using a two-sensing-finger microgripper. *IEEE Trans. Autom. Sci. Eng.* 10(3):515–24
 116. Komati B, Clévy C, Lutz P. 2016. High bandwidth microgripper with integrated force sensors and position estimation for the grasp of multistiffness microcomponents. *IEEE/ASME Trans. Mechatron.* 21(4):2039–49
 117. Komati B. 2014. *Automated microassembly using an active microgripper with sensorized end-effectors and hybrid force/position control*. PhD Thesis, Univ. Franche-Comté, Besançon, Fr.
 118. Rakotondrabe M, Ivan IA, Khadraoui S, Lutz P, Chaillet N. 2014. Simultaneous displacement/force self-sensing in piezoelectric actuators and applications to robust control. *IEEE/ASME Trans. Mechatron.* 20(2):519–31
 119. Boudaoud M, Gaudenzi De Faria M, Haddab Y, Haliyo S, Le Gorrec Y, et al. 2015. Robust microscale grasping through a multimodel design: synthesis and real time implementation. *Control Eng. Pract.* 39:12–22
 120. Flores G, Rakotondrabe M. 2023. Classical Bouc-Wen hysteresis modeling and force control of a piezoelectric robotic hand manipulating a deformable object. *IEEE Cont. Syst. Lett.* 7:2413–18
 121. Li Z, Fu P, Wei BT, Wang J, Li AL, et al. 2022. An automatic drug injection device with spatial micro-force perception guided by an microscopic image for robot-assisted ophthalmic surgery. *Front. Robot. AI* 9:913930
 122. Li T, King NKK, Ren H. 2020. Disposable FBG-based tridirectional force/torque sensor for aspiration instruments in neurosurgery. *IEEE Trans. Ind. Electron.* 67(4):3236–47
 123. Tiwari B, Clévy C, Lutz P. 2019. High-precision gluing tasks based on thick films of glue and a microrobotics approach. *IEEE Robot. Autom. Lett.* 4(4):4370–77
 124. Shi B, Wang F, Huo Z, Tian Y, Cong R, Zhang D. 2022. Contact force sensing and control for inserting operation during precise assembly using a micromanipulator integrated with force sensors. *IEEE Trans. Autom. Sci. Eng.* 20(3):2147–55
 125. Liu S, Xu D, Zhang D, Zhang Z. 2014. High precision automatic assembly based on microscopic vision and force information. *IEEE Trans. Autom. Sci. Eng.* 13(1):382–93
 126. Zhao G, Teo CL, Hutmacher DW, Burdet E. 2010. Force-controlled automatic microassembly of tissue engineering scaffolds. *J. Micromech. Microeng.* 20(3):35001
 127. Kim DH, Kim B, Kang H. 2004. Development of a piezoelectric polymer-based sensorized microgripper for microassembly and micromanipulation. *Microsyst. Technol.* 10(4):275–80

128. Nguyen TV, Tani R, Takahata T, Shimoyama I. 2019. Development of a single-chip elasticity sensor using MEMS-based piezoresistive cantilevers with different tactile properties. *Sens. Actuators A* 285:362–68
129. Nan Z, Xu Q, Zhang Y, Ge W. 2019. Force-sensing robotic microinjection system for automated multi-cell injection with consistent quality. *IEEE Access* 7:55543–53
130. Esfahani AM, Minnick G, Rosenbohm J, Zhai H, Jin X, et al. 2022. Microfabricated platforms to investigate cell mechanical properties. *Med. Novel Technol. Devices* 13:100107
131. Govilas J, Guicheret-Retel V, Amiot F, Beaugrand J, Placet V, Clévy C. 2022. Platen parallelism significance and control in single fiber transverse compression tests. *Composites A* 159:106990
132. André AN, Lehmann O, Govilas J, Laurent GJ, Saadana H, et al. 2024. Automating robotic micro-assembly of fluidic chips and single fiber compression tests based-on Θ visual measurement with high-precision fiducial markers. *IEEE Trans. Autom. Sci. Eng.* 21:353–66

